BMC Biology

RESEARCH ARTICLE

Open Access

CD4$^+$ and CD8$^+$ regulatory T cell characterization in the rat using a unique transgenic *Foxp3-EGFP* model

Séverine Ménoret[1,2*], Laurent Tesson[2], Séverine Remy[2], Victor Gourain[1], Céline Sérazin[2], Claire Usal[2], Aude Guiffes[2], Vanessa Chenouard[2], Laure-Hélène Ouisse[2], Malika Gantier[2], Jean-Marie Heslan[2], Cynthia Fourgeux[2], Jeremie Poschmann[2], Carole Guillonneau[2] and Ignacio Anegon[2*]

Abstract

Background Regulatory T cells (Treg) in diverse species include CD4$^+$ and CD8$^+$ T cells. In all species, CD8$^+$ Treg have been only partially characterized and there is no rat model in which CD4$^+$ and CD8$^+$ FOXP3$^+$ Treg are genetically tagged.

Results We generated a *Foxp3-EGFP* rat transgenic line in which *FOXP3* gene was expressed and controlled EGFP. CD4$^+$ and CD8$^+$ T cells were the only cells that expressed EGFP, in similar proportion as observed with anti-FOXP3 antibodies and co-labeled in the same cells. CD4$^+$EGFP$^+$ Treg were 5–10 times more frequent than CD8$^+$EGFP$^+$ Treg. The suppressive activity of CD4$^+$ and CD8$^+$ Treg was largely confined to EGFP$^+$ cells. RNAseq analyses showed similarities but also differences among CD4$^+$ and CD8$^+$ EGFP$^+$ cells and provided the first description of the natural FOXP3$^+$CD8$^+$ Treg transcriptome. In vitro culture of CD4$^+$ and CD8$^+$ EGFP$^-$ cells with TGFbeta and IL-2 generated induced EGFP$^+$ Treg. CD4$^+$ and CD8$^+$ EGFP$^+$ Treg were expanded upon in vivo administration of a low dose of IL-2.

Conclusions This new and unique rat line constitutes a useful model to identify and isolate viable CD4$^+$ and CD8$^+$ FOXP3$^+$ Treg. Additionally, it allows to identify molecules expressed in CD8$^+$ Treg that may allow to better define their phenotype and function not only in rats but also in other species.

Keywords Immune tolerance, Genome editing, Gene knockin, Foxp3, CD4+ Treg, CD8+ Treg

Background

Regulatory T cells (Treg) play a central role in controlling immune effector mechanisms [1–3]. Both CD4$^+$ and CD8$^+$ Treg have been repeatedly described in humans, non-human primates, and rodents [3–5]. CD4$^+$FOXP3$^+$ Treg can be natural (nTregs), i.e., physiologically developed in the thymus and that migrate to the periphery [3]. The existence of natural CD8$^+$FOXP3$^+$ Treg has not been yet formally demonstrated [4]. At the same time, CD4$^+$ and CD8$^+$FOXP3$^+$ Treg can be induced from FOXP3$^-$ T (iTreg) in pathophysiological situations or following treatments, either in vivo or in vitro [1, 3, 4, 6, 7]. Additionally, there are also CD4$^+$ and CD8$^+$ iTreg that are FOXP3$^-$ [1, 4, 8]. The FOXP3 transcription factor is essential for the function of canonical natural CD4$^+$ Treg [1]. CD8$^+$ Treg is and heterogeneous cell population [9, 10], as CD4$^+$ Treg, but the phenotype and function of

*Correspondence:
Séverine Ménoret
severine.menoret@univ-nantes.fr
Ignacio Anegon
ianegon@nantes.inserm.fr
[1] Nantes Université, CHU Nantes, Inserm, CNRS, SFR Santé, Inserm UMS 016 CNRS UMS 3556, F-44000 Nantes, France
[2] INSERM, Centre de Recherche en Transplantation et Immunologie UMR1064, Nantes Université, Nantes, France

natural $CD8^+FOXP3^+$ Treg is less well defined than for $CD4^+FOXP3^+$ Treg [4]. CD8+ Foxp3+ Treg cells have been previously identified in human tonsils [11] and in blood of HIV-infected patients [12]. We and others have described in rats and humans a population of cells $CD8^+$ Treg that is defined by the low or absent expression of CD45RC ($CD8^+CD45RC^{low/-}$) [7, 13–16]. In mice, although CD45RC has been used to purify $CD4^+$ and $CD8^+$ [17], Treg little characterization of these cells has been done. In rats and humans, all $CD4^+$ and $CD8^+$ Treg suppressive activity is comprised among the $CD45RC^{low/-}$ fraction, but the $FOXP3^+$ cells are only a small fraction of this population. Although $CD4^+$ Treg in all species are comprised in the $CD25^{high}CD127^{low}$ fraction of $CD45RC^{low/-}$ cells, for $CD8^+$ Treg, there is no consensus on the markers useful to further refine the analysis of the $CD45RC^{low/-}$ population and to analyze if the suppressive activity is exclusively within the $FOXP3^+$ fraction [4, 7].

Mouse $FOXP3^+CD4^+$ Treg have been extensively analyzed using transgenic animals in which the *Foxp3* promoter controls reporter genes [18–24] allowing the sorting of viable $CD4^+$ reporter gene$^+$ Treg. $CD8^+FOXP3^+$ cells were identified in these mice but an in-depth analysis of their phenotype and function was not reported [19–22].

Rat $CD4^+$ and $CD8^+$ Treg are in general less well defined than human and mouse Treg and comparison of Treg among different species are very rare and only on the T $CD4^+$ lineage [5]. There is no description of rat transgenic lines that allow to define $FOXP3^+$ cell lineages.

The immune system of rats have several characteristics that make them more similar to humans than mice, such as expression of MHC-II molecules by T cells, CD4 expression by a subset of DCs and normal levels of complement [25, 26]. Additionally, certain human immune diseases are better modelized in rat than in mouse models with the same genetic mutations [26], such as for ankylosing spondylopathy [27] and autoimmune polyendocrinopathy candidiasis ectodermal dystrophy (APECED) [28], in *HLA-B27* transgenic and in *Aire* knockout rats, respectively.

Thus, there is need to better define Treg in the rat, specially the $CD8^+$ Treg population and to dispose of animals with Foxp3-tagged Treg that can be used to study Treg in different situations.

Using CRISPR/Cas9 and transgenic technologies, we generated a rat line with a knockin of EGFP in the 3′ of the *Foxp3* gene allowing the natural expression of FOXP3 from the targeted allele with the expression of EGFP under the control of the endogenous *Foxp3* promoter. The phenotype, suppressive function, and transcriptomic of both $CD4^+$ and $CD8^+$ $EGFP^+$ Treg were analyzed. The transcriptomic analysis of $CD8^+EGFP^+$ Treg is to the best of our knowledge the first one to be described. Using EGFP as a marker′ we show expansion of both $CD4^+$ and $CD8^+$ Treg following IL-2 treatment in vivo and generation of iTreg in vitro.

Results

Generation of transgenic rats with EGFP knockin into the *Foxp3* gene

To mark FOXP3-expressing cells we inserted the EGFP coding sequence in-frame and before the stop codon of the *Foxp3* gene (Fig. 1A). EGFP was preceded by a T2A sequence that allowed self-splicing of a monocistronic *Foxp3-EGFP* mRNA. Thus, *Foxp3*-expressing cells will show simultaneous and independent expression of FOXP3 and EGFP under the control of the endogenous *Foxp3* promoter (referred to as *Foxp3-EGFP* rats below).

Rat zygotes were microinjected and were transferred ($n = 148$) into pseudopregnant females. Newborns ($n = 25$) were genotyped by PCR followed by sequencing and one founder was identified as a KI (Fig. 1B), whereas other founders ($n = 4$) showed indels (data not shown).

This founder was mated with a wild-type partner and a *Foxp3-EGFP* rat line was stably generated with a Mendelian segregation of the *Foxp3-EGFP* allele (data not shown).

EGFP was only expressed by $CD8^+$ and $CD4^+$ Treg

Cytofluorimetric analysis of the lymph nodes, thymus, spleen, blood, and bone marrow showed that a proportion of TCR^+CD4^+ or TCR^+CD8^+ cells expressed EGFP that was equivalent to the proportion of $FOXP3^+$ cells detected using an anti-FOXP3 antibody (Fig. 2 and supplementary Fig. 1). TCR^- or NK cells did not express EGFP (Fig. 2; Additional file 1: Fig. S1A). Analysis of homozygote *Foxp3-EGFP* animals showed comparable expression of FOXP3 as detected using the anti-FOXP3 antibody and all $FOXP3^+$ were also $EGFP^+$ while none of the $FOXP3^+$ cells were $EGFP^-$ (Additional file 1: Fig. S1B). Of note, permeabilization and fixation of cells required to analyze FOXP3 using antibodies reduced the expression of EGFP, as already described [29] (Additional file 1: Fig. S1B). Thus, to further confirm these results, we sorted $EGFP^+$ and $EGFP^-$ cells and analyzed the expression of FOXP3. Again, the percentage of cells expressing both EGFP and FOXP3 matched (Additional file 1: Fig. S1C), indicating not only faithful expression of EGFP from the *Foxp3* promoter but also that expression of FOXP3 was not impaired by the insertion of the EGFP sequence.

A quantitative analysis of $CD4^+EGFP^+$ T cells in thymus and spleen ranged in percentage between 5 and 10% of the cells, respectively (Table 1). In absolute numbers,

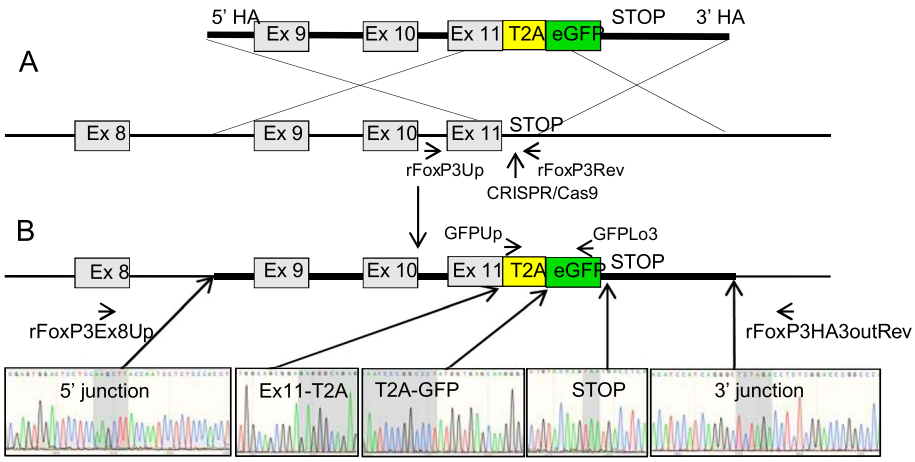

Fig. 1 Schematic representation of the GFP KI strategy and genotyping of potential *Foxp3-EGFP* founders. **A** (upper diagram) A double stranded DNA donor was generated containing a EGFP sequence preceded by a self-splicing T2A sequence both flanked in 5′ and 3′ ′homology arms for the indicated *Foxp3* sequences (lower diagram). Upon microinjection of a sgRNA designed to recognize a DNA sequence immediately 3′ of the stop codon, Cas9 protein and donor DNA, cleavage of the *Foxp3* gene favors homologous-recombination of the donor DNA sequences. **B** (upper diagram) Schematic representation of EGFP under the transcriptional control of an intact *Foxp3* gene. Both FOXP3 and EGFP will be generated as independent proteins through self-splicing imposed by the T2A sequence (lower diagram) Sanger sequences of a founder in which in-frame junctions are present between the 5′ and 3′ homology arms of the DNA donor and the *Foxp3* gene as well as the entire donor DNA sequence is conserved with conserved junctions between exon 11-T2A, T2A-EGFP, and EGFP-stop sequences. Primers used for the different PCR sequences are outlined

$CD4^+EGFP^+$ T cells ranged between 8×10^4 and 2.2×10^6 cells per ml of blood and in the spleen, respectively (Table 1). $CD8^+EGFP^+$ T cells represented roughly 10% of the $CD4^+EGFP^+$ cells and ranged between 0.6 and 1.3% of the cells in the thymus and lymph nodes, respectively (Table 1). In absolute numbers, $CD8^+EGFP^+$ cells ranged between 0.7×10^4 and 0.4×10^6 cells per ml of blood and in lymph nodes, respectively (Table 1).

Thus, *Foxp3-EGFP* rats appear to be a faithful tool to identify and analyze $CD4^+$ and $CD8^+$ Treg.

Phenotype and lymphoid organ distribution of $TCR^+CD4^+EGFP^+$ and $TCR^+CD8^+EGFP^+$ Treg

$CD4^+CD25^{high}CD127^{low/neg}$ Treg cells, a phenotype largely belonging to $CD4^+FOXP3^+$ Treg in humans, mice, and rats [5], were largely $EGFP^+$, whereas $CD4^+CD25^-CD127^+$ Tconv cells were largely $EGFP^-$ (Fig. 3A). $CD8^+CD25^{high}CD127^{low/neg}$ were also largely $EGFP^+$, whereas $CD8^+CD25^-CD127^+$ cells were largely $EGFP^-$ (Fig. 3A). Using CD45RC, a marker that has been used both for $CD4^+$ and $CD8^+$ Treg in rats and humans [13, 15, 16], $EGFP^+$ cells were detected mostly among $CD45RC^-$ $CD4^+$ and $CD8^+$ T cells but also in a lesser proportion in $CD4^+CD45RC^{low}$ cells but never among $CD45RC^{high}$ cells (Fig. 3B).

The markers CD25, MHC-II, CD28, and CD44 were more and CD62L less expressed in both $CD4^+$ and $CD8^+EGFP^+$ vs. $EGFP^-$ cells (Fig. 3C). CD5 and CD26 were equally expressed by all cell subtypes (data not shown).

The proportion and absolute numbers of $TCR^+CD4^+EGFP^+$ Treg vs. $TCR^+CD8^+EGFP^+$ Treg were ~10-fold higher in the thymus, blood, spleen, and bone marrow and ~5-fold higher in lymph nodes (Table 1).

We compared the frequency of $TCR^+CD4^+EGFP^+$, $TCR^+CD8^+EGFP^+$ × and EGFP expression levels Treg in rats to the ones in mice also harboring EGFP in the 3′ end of the *Foxp3* gene, and thus as in *Foxp3-EGFP* rats, controlled by the *Foxp3* endogenous promoter [18]. The frequency of $TCR^+CD4^+EGFP^+$ cells in rats vs. mice in different immune compartments showed similar percentage in the spleen, lymph nodes and bone marrow and higher in the blood (Additional file 1: Table S1). $TCR^+CD8^+EGFP^+$ cells were increased in

(See figure on next page.)

Fig. 2 Flow cytometry analysis of peripheral blood lymphocyte and lymph node cells from *Foxp3-EGFP* rats. **A** Blood and **B** axillary lymph nodes were harvested from 12-week-old *Foxp3-EGFP* or wild-type (WT) rats, and single-cell suspensions were gated by SSC and FSC on lymphocytes followed by the identification with mAbs of major cell populations; TCR^+ cells (TCR^+CD4^+, TCR^+CD8^+), TCR^- cells (TCR^-CD4+ and TCR^-CD8+), and $CD161^{high}$ in total cells for NK cells. These populations were then analyzed for FOXP3 expression by EGFP expression and by using an anti-FOXP3 mAb. For both **A** and **B**, upper panels with contour plots representative from one animal and lower graphs the mean and SEM of all animals analyzed. Student's *t* test $*P < 0.05$, $**P < 0.01$, $***P < 0.001$, and $****P < 0.0001$

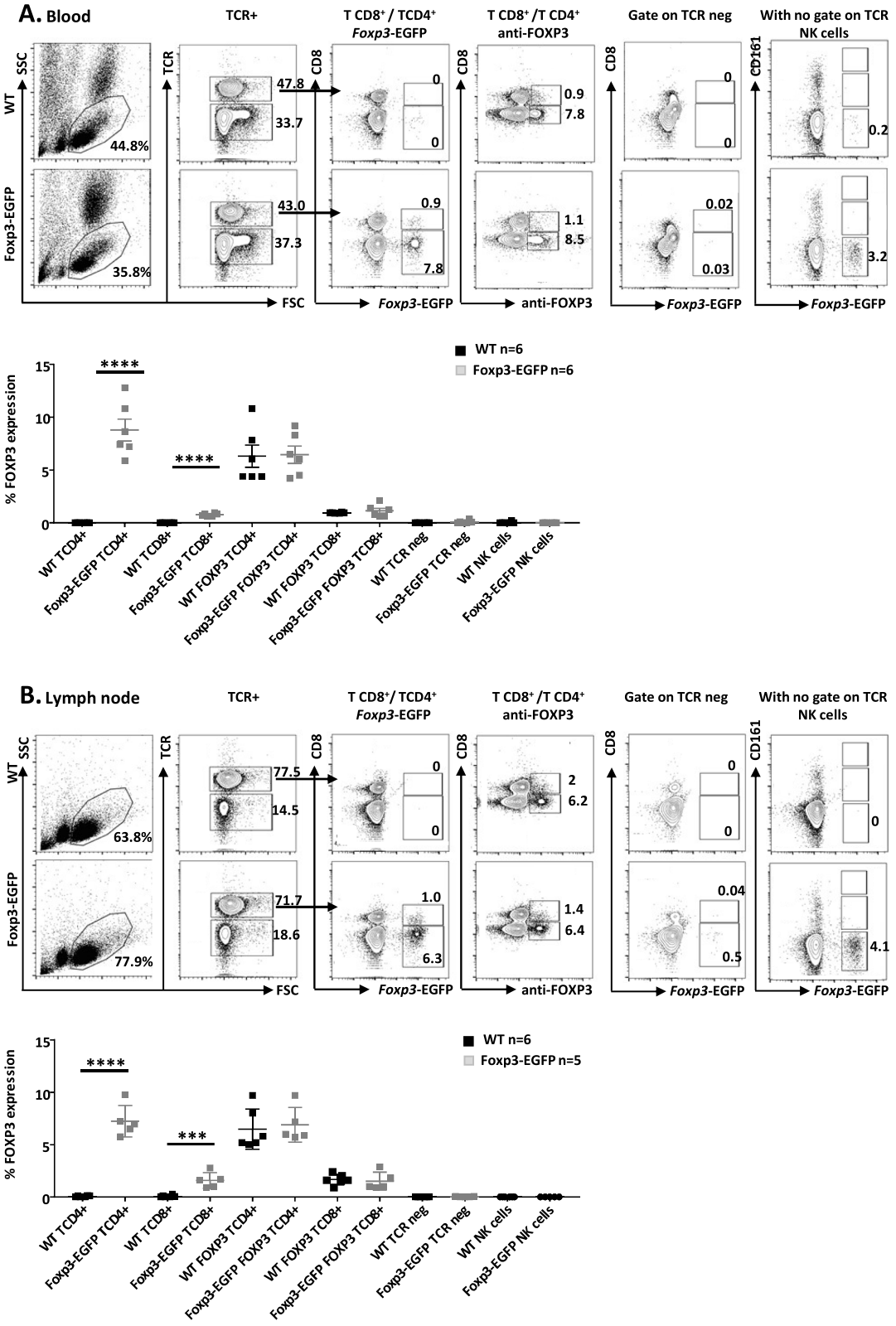

Fig. 2 (See legend on previous page.)

Table 1 Quantification of $CD4^+$ and $CD8^+$ Treg in different immune compartments

	Units	Thymus	LN	Spleen	BM	Blood/ml
$CD4^+EGFP^+$ ($n = 5$)	% [a]	5.2 ± 0.9	7.8 ± 1.7	10 ± 0.2	7.2 ± 3	7.9 ± 0.6
	cells × 10^6	2.24 ± 1	0.4 ± 0.1	2.2 ± 0.4	0.19 ± 0.004	0.083±0.03
$CD8^+EGFP^+$ ($n = 5$)	% [b]	0.6 ± 0.15	1.3 ± 0.4	0.7 ± 0.01	0.8 ± 0.45	0.7 ± 0.1
	cells × 10^6	0.28 ± 0.2	0.4 ± 0.6	0.16 ± 0.02	0.003 ± 0.002	0.007 ± 0.002

LN axillar lymph nodes, *BM* bone marrow from1 femur/animal

[a] Among TCR^+CD4^+

[b] Among TCR^+CD8^+

rats vs. mice in the spleen but not in the blood, lymph nodes, and bone marrow (Additional file 1: Table S1 A). Although the intensity of EGFP expression was significantly higher in *Foxp3-EGFP* rats vs. *Foxp3-EGFP* mice (Additional file 1: Table S1 B), and this could have explained these differences, the percentages of $FOXP3^+$ Treg defined with anti-FOXP3 antibodies and EGFP in *Foxp3-EGFP* mice were not different (Additional file 1: Fig. S7).

Overall, $EGFP^+$ cells are largely confined to Treg populations defined by markers as $CD25^{high}$, $CD127^{low/neg}$ and $CD45RC^{low/neg}$. $CD4^+EGFP^+$ Treg are present in higher numbers than $CD8^+EGFP^+$ Treg.

In vitro suppressive function of $EGFP^+$ and $EGFP^-$ fractions of CD4+ and CD8+ Treg

We then aimed to confirm the suppressive function of $CD4^+$ and $CD8^+$ $EGFP^+$ Tregs by using a suppressive assay of T cell proliferation. Present cell surface markers identifying $CD8^+$ Tregs are less discriminative than for $CD4^+$ Tregs. Since $CD8^+CD45RC^{low/-}$ and not $CD8^+CD45RC^{high}$ T cells contain most of the suppressive activity among $CD8^+$ cells both in rats [4] and humans [7], we sorted $CD8^+CD45RC^{low/-}$ cells either $EGFP^+$ or $EGFP^-$ and compared their suppressive function. Although $CD4^+CD25^+CD127^{low}$ Tregs contain a very small fraction of $EGFP^-$ cells, to keep the same strategy of analysis for $CD4^+$ and $CD8^+$ Tregs, we sorted $CD4^+CD25^{high}CD127^{low}$ cells $EGFP^+$ or $EGFP^-$ fractions and compared their suppressive activity. The suppressive activity was confined to the $EGFP^+$ fraction for both the $CD8^+CD45RC^{low/-}$ and $CD4^+CD25^{high}CD127^{low}$ Tregs (Fig. 4 and Additional file 1: Fig. S2).

Thus, isolation of viable $CD4^+$ and $CD8^+$ Treg by their expression of EGFP allows to explore their suppressive function.

Transcriptomic analyses of natural and induced $EGFP^+$ $CD8^+$ and $CD4^+$ Treg

To gain further insight into the molecular properties of $CD4^+$ and $CD8^+$ Treg, we sorted $CD25^{high}CD127^{low}CD4^+EGFP^+$, $CD25^{high}CD127^{low}CD4^+EGFP^-$, $CD45RC^{low/-}CD8^+EGFP^+$, and $CD45RC^{low/-}CD8^+EGFP^-$ cells and compared their transcriptomic profiles. Principal components analysis (PCA) showed that CD4+EGFP+ vs. CD4+EGFP- (Fig. 5A left) and CD8+EGFP+ vs. CD8+EGFP- T cells (Fig. 5A middle) appeared to be distinct with a confidence of 95% as shown by ellipses. This was in contrast to the CD4+EGFP+ and CD8+EGFP+ T cells which showed no clear distinction (Fig. 5A right).

Comparison gene expression revealed multiple differentially expressed genes (DEG) between the different cell types (FDR Q-value < 0.05) (Fig. 5B). When comparing $CD4^+EGFP^+$ vs. $CD4^+EGFP^-$ cells, $CD4^+EGFP^+$ cells had 309 genes with higher expression. Among them were several Treg specific genes (e.g., *Foxp3*, *Ikzf2*, *Tox*, *Lrrc32(GARP)).* Whereas $CD4^+EGFP^-$ cells had 290 genes upregulated with some genes with a $CD4^+$ Th cell specific expression (e.g., *Nkg7*, *Gzmb*, *Cd40lg*…) (Fig. 5B left, Additional file 1: Table S2). Comparison of $CD8^+EGFP^+$ vs. $CD8^+EGFP^-$ cell, revealed that $CD8^+EGFP^+$ cells had 373 genes with

(See figure on next page.)

Fig. 3 Phenotype of $EGFP^+$ cells. Single-cell suspensions were obtained from spleen from a *Foxp3-EGFP* rat, lymphocytes gated by SSC/FSC and analyzed for the phenotype of $CD4^+$ and $CD8^+$ $EGFP^+$ cells. **A** TCR^+ cells were labeled with an anti-CD8alpha mAb to identify $CD8^+$ and $CD8^-$/$CD4^+$ and analyzed for CD25 and CD127 expression followed by EGFP detection. **B** TCR^+CD4^+ or TCR^+CD8^+ cells were analyzed for CD45RC expression, levels identifying high (H), low (L), and negative (N) cells and EGFP expression in these populations. **C** Histograms of $TCR^+CD4^+EGFP^+$, TCR+CD4+$EGFP^-$, TCR+CD8+EGFP+, and $TCR^+CD8^+EGFP^-$ cells analyzed with the indicate mAbs. Percentages above the traits correspond to the number of positive cells above staining with isotype control mAbs. In **A**, **B**, and **C** one experiment representative of 6 performed in the same conditions. Panels with contour plots or histograms representative from one animal and right graphs the mean and SEM of all animals analyzed. Student's *t* test *$P < 0.05$, **$P < 0.01$, ***$P < 0.001$, and ****$P < 0.0001$

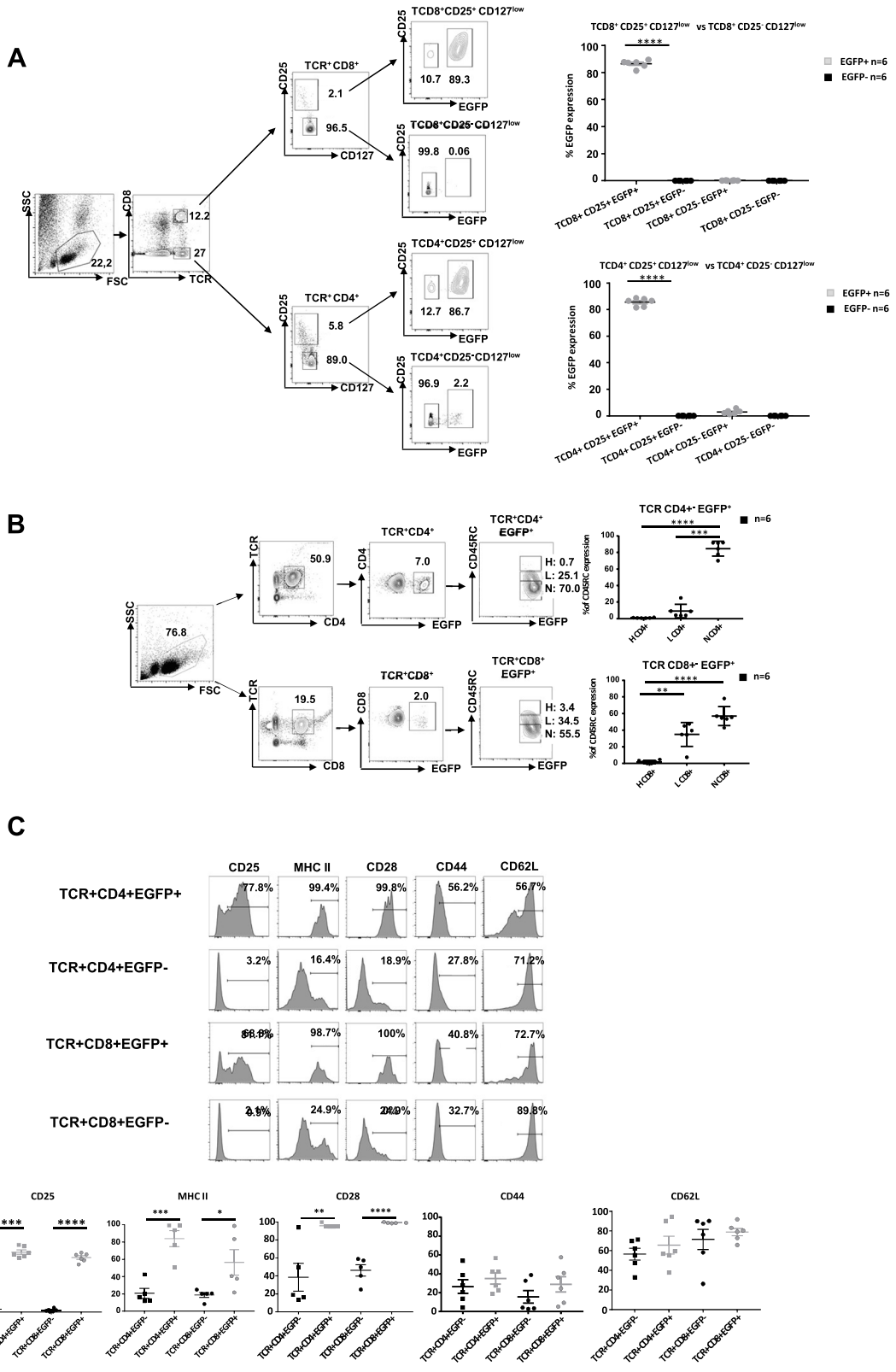

Fig. 3 (See legend on previous page.)

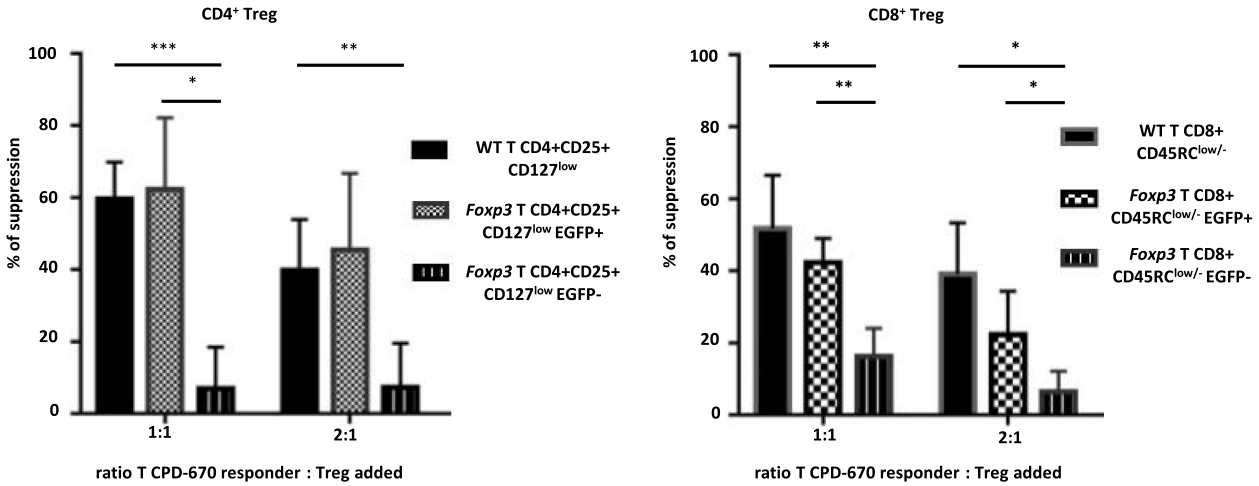

Fig. 4 Suppressive activity of TCR$^+$CD4$^+$EGFP$^+$ and TCR$^+$CD8$^+$EGFP$^+$ cells in an MLR. An MLR was performed by co-culturing in a 1:1 ratio spleen CD4$^+$CD25$^-$ Tconv cells from SD/Crl rats (MHC haplotype u) with enriched spleen APCs from Lewis 1A (MHC haplotype a) rats. Spleen Tregs from wild-type (WT) or *Foxp3-EGFP* SD/Crl rats were sorted based on their surface phenotype using previously defined markers. For CD4$^+$ Tregs, TCR$^+$CD4$^+$CD25$^+$CD127$^{low/-}$ and for CD8$^+$ Tregs, TCR$^+$CD8$^+$CD45RC$^{low/-}$. CD4$^+$ and CD8$^+$ Tregs were then sorted based on the expression or not of EGFP. The four populations of Tregs, CD4$^+$EGFP$^+$, and EGFP$^-$ as well as CD8$^+$EGFP$^+$ and EGFP$^-$ were added to the MLR in a 1:1 or 1:2 Tregs to CDP-670 labeled Tconv cells. Values are expressed as mean % ± SEM of suppression normalized to MLR proliferation in the absence of Tregs (0% inhibition of proliferation). $n = 4$. Student's t test *$P < 0.05$, **$P < 0.01$, ***$P < 0.001$, and ****$P < 0.0001$

higher expression, again with genes that are specific to Treg such as (e.g., *Foxp3*, *Lrrc32*(GARP), *Il2ra*) but others not (e.g., *C1qa* and *C1qc*) whereas CD8$^+$EGFP$^-$ cells 363 genes upregulated, such as genes critical for the cytotoxic function of effector *CD8*$^+$ T (e.g., *Gzmk*, *Gzmm..*) (Fig. 5B middle, Additional file 1: Table S3). When comparing CD4$^+$EGFP$^+$ vs. CD8$^+$EGFP$^+$ cells, CD4$^+$EGFP$^+$ cells upregulated 322 genes, such as *Gm2a*, *Smpdl3a* and *Nrp1.* CD8$^+$EGFP$^+$ upregulated 242 genes, such as *Lag3*, *Np4*, *C1qa*, and *Tnfrsf18* (Fig. 5B right, Additional file 1: Table S4).

Heatmap analysis of DEG grouped together with different transcriptomic profiles all CD4$^+$EGFP$^+$ vs. CD4$^+$EGFP$^-$ cells, CD8$^+$EGFP$^+$ vs. CD8$^+$EGFP$^-$ cells, as well as CD4$^+$EGFP$^+$ cells vs. CD8$^+$EGFP$^+$ cells (Additional file 1: Fig. S3). Among these DEG, many were genes of the immune system, and for CD4$^+$EGFP$^+$ cells with a fold change of log2 fold change of > 1-fold, there were already identified key genes such as some described above as well as *Itgb8*, *Cd80*, and *Tnfrsf9* (Additional file 1: Table S2) [30–34].

For CD8$^+$EGFP$^+$ cells with a log2 fold change of > 1-fold, there were genes shared with CD4$^+$EGFP$^+$ Treg such as some described above as well as *Il4r*, *Fcna*, and *Art2b* as well as others previously described in human or mouse CD4$^+$ Treg, such as *Il2ra*, *Lgmn* [35], and *Tnfrsf9* (Additional file 1: Table S3).

We then compared upregulated genes with immune functions in CD4$^+$EGFP$^+$ vs. CD8$^+$EGFP$^+$ Treg (Supplementary Table 4). In CD4$^+$EGFP$^+$ Treg, we observed increased expression of genes such as *MHC-II (LOC688090)*, *Lrrc32*, *Ccr6*, *Selplg*, and *Tnfrsf4* (Additional file 1: Table S4). In CD8$^+$EGFP$^+$ Treg, we observed upregulation of genes with immune function not previously linked to Treg, such as *Fcna*, *Hmox1*, *Spic*, and complement pathway genes (*C1qc*, *C1qa*, and *C1qb)* (Additional file 1: Table S4). Further analysis of expression levels of selected immune genes in individual samples of the four populations of cells showed that some were upregulated in both CD4$^+$EGFP$^+$ and CD8$^+$EGFP$^+$ populations vs. the EGFP$^-$ counterparts, such as *Foxp3*, *Lrrc32*, *Tnfrsf1b*, *Tnfrsf9*, *Il2ra*, *Tox*, and *Il4r*, whereas others were only upregulated in CD4$^+$EGFP$^+$ Treg, such as *Stap2* and *Igtb8*, or in CD8$^+$EGFP$^+$ Treg, such as *Timp1* and *Erc1* (Additional file 1: Fig. S4A).

Based on the genes differently expressed and the biological pathways in which they are involved, we determined 4 principal processes with different pathways and with differential involvement for each cell type: immune cells activation, proliferation, and adhesion as well as a miscellaneous one (Additional file 1: Fig. S4B). CD4$^+$EGFP$^+$ vs. CD4$^+$EGFP$^-$ cells, expressed genes involved in immune cell activation and adhesion but not in immune cell proliferation and several of these pathways were shared with CD8$^+$EGFP$^+$ Treg. CD8$^+$EGFP$^+$ vs. CD8$^+$EGFP$^-$ cells also expressed genes involved in immune cell proliferation or its regulation. CD4$^+$EGFP$^+$ vs. CD8$^+$EGFP$^+$ showed genes involved in the miscellaneous pathways, such as Th1 and Th2 cell differentiation and regulation of inflammatory responses.

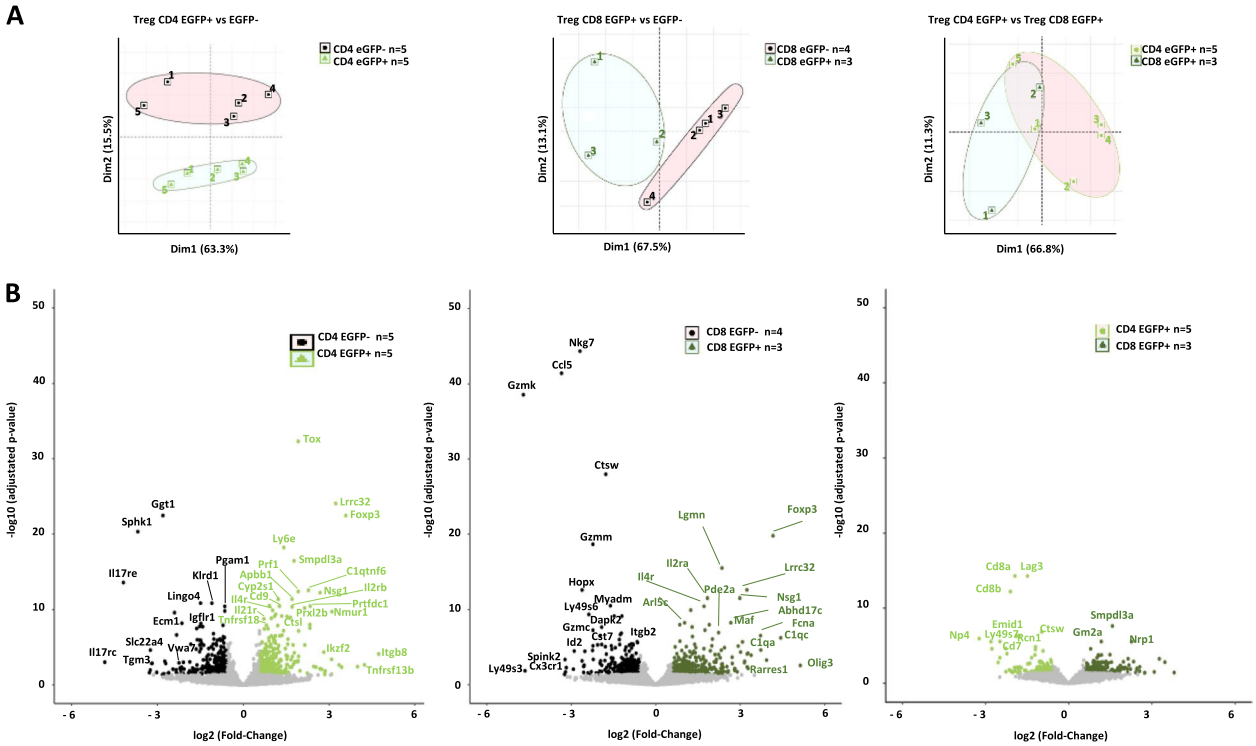

Fig. 5 RNAseq analyses of EGFP$^+$ and EGFP$^-$ within CD4$^+$ and CD8$^+$ T cells. TCR$^+$CD25^{high}CD127^{low}CD4$^+$ and TCR$^+$CD45RC$^{low/-}$ EGFP$^+$ and EGFP$^-$ T cells were cell sorted and RNAseq analyses were performed comparing CD4$^+$EGFP$^+$ vs. CD4$^+$EGFP$^-$ cells (left column), and CD8$^+$EGFP$^+$ vs. CD8$^+$EGFP$^-$ cells (middle column) and CD8$^+$EGFP$^+$ vs. CD4$^+$EGFP$^+$ cells right column. **A** Principal components analysis (PCA) of all samples and of expressed genes. **B** Volcano plots. (Left) Light green indicates overexpression in CD4$^+$EGFP$^+$ vs. CD4$^+$EGFP$^-$ cells and black of CD4$^-$EGFP$^+$ vs. CD4$^+$EGFP$^+$ cells. (Middle) Dark green indicates overexpression in CD8$^+$EGFP$^+$ vs. CD8$^+$EGFP$^-$ cells and black of CD8$^-$EGFP$^+$ vs. CD8$^+$EGFP$^+$ cells. (Right) Light green indicates overexpression in CD4$^+$EGFP$^+$ vs. CD8$^+$EGFP$^+$ cells and dark green of CD8$^-$EGFP$^+$ vs. CD4$^+$EGFP$^+$ cells. **C** Heatmaps of all differentially expressed genes. Low expression levels are in blue, mean expression levels are in white, and high expression levels are in red. Each sample number is depicted on the top

Venn analyses of all genes upregulated by CD4$^+$EGFP$^+$ vs. CD8$^+$EGFP$^+$ Treg vs. their EGFP$^-$ counterparts as well as between the two Treg populations allowed to define genes that were unique and common among them (Additional file 1: Fig. S4C). The genes upregulated and downregulated in the Venn diagrams are listed in Supplementary Tables 5 and 6, respectively.

We finally confirmed at the protein level some of the genes that were upregulated at the RNAseq level such as for CD25/*Il2ra* (Fig. 3 and Additional file 1: Fig. S5A, respectively), as well as CD44/*Cd44* and ICOS/*Icos* (Additional file 1: Fig. S5A).

Altogether, the transcriptome data suggests in CD8$^+$EGFP$^+$ Treg common genes previously described for CD4$^+$ Treg but also many others that differ.

Analysis of in vitro generated EGFP$^+$ induced Tregs

We tested whether EGFP$^-$ Tconv cells from *Foxp3-EGFP* rats could be converted to EGFP$^+$ induced Tregs. To this end, CD4$^+$CD25$^-$ and CD8$^+$CD45RC$^{low/-}$EGFP$^-$ T cells were isolated and cultured in the presence of anti-CD3 and CD28 mAbs, IL-2 and TGFbeta. Stimulation with IL-2 in the absence of TGFbeta has been shown to induce FOXP3 in T cells that were FOXP3$^-$ in humans [36], likely as a marker of T cell activation, but not in mice [37], whereas in the presence of IL-2 and TGFbeta, FOXP3 is induced in both species [36, 37]. The induction of FOXP3 in rat T cells has not been clearly addressed. In the presence of anti-CD3 and anti-CD28 and TGFbeta alone, CD4$^+$CD25$^-$EGFP$^-$ and CD8$^+$CD45RC^{low}EGFP$^-$ T cells converted to 19.7% and 7.9% of EGFP$^+$ induced Tregs, respectively, and the MFI expression of EGFP was very similar than the one of EGFP$^+$ natural Tregs (for CD4$^+$EGFP$^+$: 9711 vs. 8394, respectively and for CD8$^+$EGFP$^+$ 11000 vs. 13000, respectively) (Fig. 6A). The expression of FOXP3 by virtually all CD4$^+$ or CD8$^+$ EGFP$^+$ cells was confirmed using anti-FOXP3 antibodies in EGFP$^+$ sorted cells following permeabilization and fixation (Additional file 1: Fig. S6). The culture

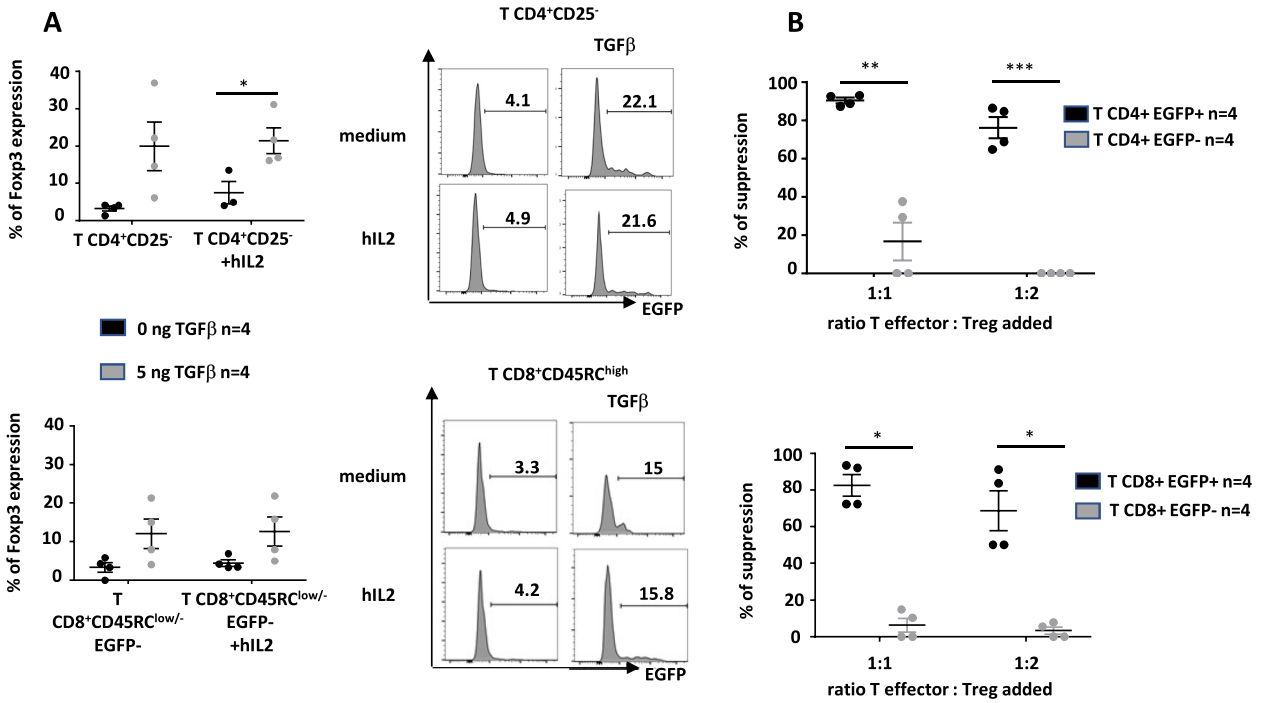

Fig. 6 Conversion of EGFP$^-$ T cells in EGFP$^+$ induced Treg. Spleen cells from *Foxp3*-EGFP animals were used to sort Tconv CD4$^+$CD25$^-$EGFP$^-$ Treg and T CD8$^+$CD45RC$^{low/-}$EGFP$^-$ cells, labeled them with CPD-670 and cultured for 3 days in the presence of anti-CD3/CD28 mAbs, IL-2 and in the absence or presence of hTGFbeta. **A** Cells that proliferated (CPD-670low/neg) were then analyzed for EGFP expression. Left graphs show mean ± SEM of 3 different experiments and right histograms show one representative analysis. **B** Suppressive assays using EGFP$^+$ (CD4$^+$ or CD8$^{+)}$ vs. EGFP$^-$ cells (CD4$^+$ or CD8$^+$) from the same cultures at different ratios with CD4$^+$ Tconv responder cells. $n = 4$, mean ± SEM. Student's *t* test $^*P < 0.05$, $^{**}P < 0.01$, $^{***}P < 0.001$, and $^{****}P < 0.0001$

with IL-2 alone or IL-2 and TGF beta did not further increase the percentage of EGFP+ cells compared to culture medium alone or TGF-beta alone, respectively (Fig. 6A).

We then evaluated the suppressive activity of the induced EGFP$^+$ Tregs from the condition in the presence of TGFbeta and IL-2 vs. the T cells from the same cultures that were EGFP$^-$. Induced CD4$^+$ and CD8$^+$ EGFP$^+$ Tregs were highly suppressive of MLR proliferation and significantly more than EGFP$^-$ cells from the same cultures that only suppressed MLRs marginally (Fig. 6B).

In conclusion, these results suggest that the use of *Foxp3-EGFP* rats allowed to define in vitro conditions of generation of induced Treg and to demonstrate that both T CD4$^+$ and CD8$^+$ lineages could generate induced Treg.

IL-2 induced expansion of EGFP$^+$ Tregs in vivo

In vivo injection of low doses of IL-2 has been shown to preferentially expand CD4$^+$ and CD8$^+$ FOXP3$^+$ Treg in mice [3], nonhuman primates [38], and humans [39]. In rats, CD4$^+$FOXP3$^+$ Treg were increased upon administration of IL-2 and CD8$^+$FOXP3$^+$ Treg were not described [40]. We aim to define whether we could detect expansion of CD4$^+$ and CD8$^+$ EGFP$^+$ Treg upon IL-2 in vivo injection. Injection of IL-2 resulted in a significant expansion of EGFP$^+$ cells as compared to untreated rats in both the CD4$^+$ (from 5.6 ± 1.4 to 17.1 ± 0.6) and CD8$^+$ (from 2.2 ± 0.4 to 9.8 ± 0.9) T compartments as well as a decrease of the reciprocal EGFP$^-$ compartments whereas NK cells remained EGFP$^-$ (Fig. 7A). In the blood of IL-2-treated animals compared to controls, increased absolute numbers of T CD4$^+$EGFP$^+$ (19-fold) and CD8$^+$EGFP$^+$ (31-fold) cells showed a higher increase vs. T CD4$^+$EGFP$^-$ (4.4-fold) and CD8$^+$EGFP$^-$ (14-fold) cells and NK cells (10-fold) (supplementary Table 7). The proportions of T CD4$^+$ and CD8$^+$ EGFP$^+$ cells were also increased in the spleen (Additional file 1: Fig. S7). As previously shown in rodents [40–42], we used phosphorylated Stat5 (Fig. 7B) and CD25 (Fig. 7C) as markers of IL-2 activity. Both markers were increased in EGFP$^+$ cells but also in EGFP$^-$ T cells.

Thus, these results suggest that *Foxp3-EGFP* rats allow to detect increases in CD4$^+$ and CD8$^+$ Treg induced by IL-2 and potentially with other agents.

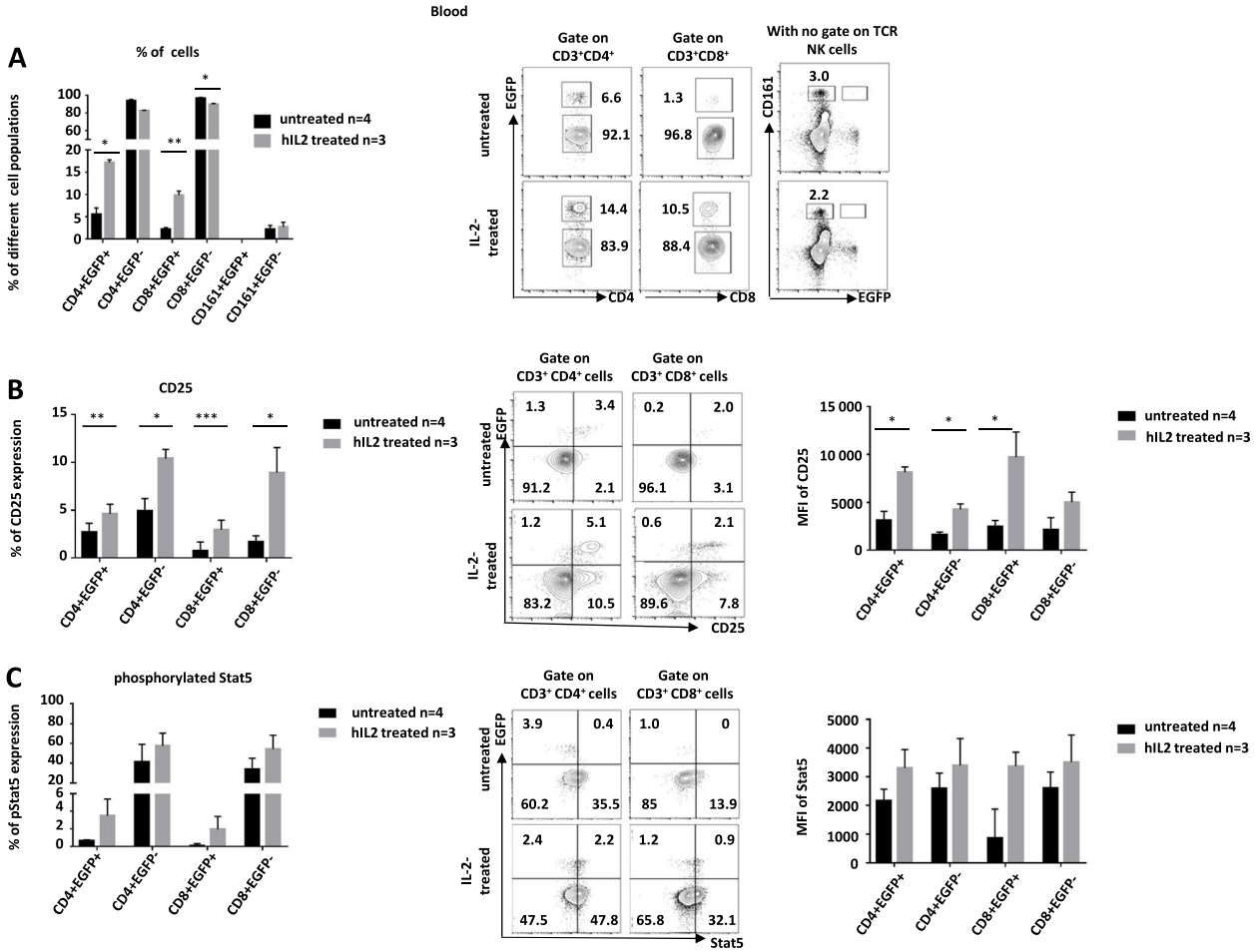

Fig. 7 IL-2 induce expansion of EGFP$^+$ Tregs in vivo. *Foxp3*-EGFP rats received or not hIL-2 and the percent of the indicated cell populations was analyzed in blood. **A** Percentages of cells in the indicated cell populations out of T cells for CD4+ and CD8+ cells and total cells for CD161 cells of IL-2-treated and untreated rats. Left graph shows mean ± SEM, $n = 3$, and right contour plots show a representative animal. **B** Percentage and MFI (left and middle histograms, respectively) of pStat5$^+$ cells in the indicated cell populations in IL-2-treated and untreated rats (mean ± SEM, $n =$ 4 or 3). Middle contour plots show a representative animal. **C** Percentage and MFI (left and middle histograms, respectively) of CD25$^+$ cells in the indicated cell populations of IL-2-treated and untreated rats (mean ± SEM, $n = 4$ or 3). Middle contour plots show a representative animal

Discussion

Foxp3-EGFP rats were generated using a strategy in which *Foxp3* gene drives the expression of EGFP placed in the 3' end of the gene. This strategy preserves Foxp3 expression of the allele in which the transgene is inserted avoiding decrease expression in heterozygous animals and also allows the use of homozygous animals to more efficiently maintain the mutated rat line. EGFP was exclusively expressed by CD4$^+$ and CD8$^+$ T cells and in proportions like the ones defined using anti-FOXP3 antibodies and thus EGFP was strictly restricted to subsets of the T cell lineage. CD4$^+$EGFP$^+$ Treg were CD25^{high}CD127$^{low/-}$CD45RC$^{low/-}$, consistent with the what has already been previously described in rats, humans, and mice. All CD8$^+$EGFP$^+$ Treg were also CD25^{high}CD127$^{low/-}$CD45RC$^{low/-}$. Quantitative analysis of *Foxp3-EGFP* rats showed that CD4$^+$EGFP$^+$ Treg were 5–10-fold more abundant than CD8$^+$EGFP$^+$ Treg.

Genetic labeling of *Foxp3*-expressing cells preserving *Foxp3* expression has been previously used in some mouse models [18, 20, 22–24]. Other mouse *Foxp3-eGFP* model generated a knockout of the allele in which GFP was inserted [19, 21]. In some of these mouse models, CD8$^+$GFP$^+$ Treg were described with frequencies ranging between 5- to 100-fold lower than CD4$^+$GFP$^+$ Treg [19–22], whereas in the others, they were not described. Analysis in our experimental conditions of CD8$^+$GFP$^+$ Treg in one of this mouse models [18] showed 9- to 130-fold more CD4$^+$EGFP$^+$ Treg vs. CD8$^+$EGFP$^+$ Treg. Rat and human FOXP3 but not mouse FOXP3 have a S422 residue (mice have a N422) that is phosphorylated upon T cell activation activation and reduces FOXP3 activity

[43]. Certain treatments can inhibit this phosphorylation and ameliorate autoimmunity in a rat model [44]. To the best of our knowledge, there are no other mammalian species with transgenic lines allowing to define FOXP3$^+$ cell lineages.

CD4$^+$ Treg defined by the usual CD25^{high} and CD127$^{low/-}$ markers showed a majority of EGFP$^+$ cells but also the presence of EGFP$^-$ cells. Analysis of their suppressive activity revealed that >90% was confined to the EGFP$^+$ fraction of cells. Similarly, CD8$^+$ Treg defined using CD45RC$^{low/-}$ as a marker also showed EGFP$^+$ and EGFP$^-$ cells and most of the suppressive activity was observed in the EGFP$^+$ vs. EGFP$^-$ fraction.

Transcriptomic analysis revealed for CD4$^+$EGFP$^+$ Treg the upregulation of genes previously described in mouse and/or human CD4$^+$ Treg as important for their differentiation, suppressive function, and oligodendrocyte regeneration, such as *Itgb8*, *Tnfrsf13b*, *Foxp3*, *Ikzf2*, *Ccn3*, *Il1rl1*, *Lrrc32*, *Cd80*, *Tnfrsf9*, *Gata3*, *Il2ra*, *Il2rb*, *Tnfrsf1b* (TNFR2 or CD120b), *Tnfrsf4* (OX40 or CD134), and *Tnfrsf18* (GITR or CD357) [30–34, 45–47]. CD4$^+$EGFP$^+$ Treg also highly upregulated genes coding with immune function not previously described for CD4$^+$ Treg, such as *Stap2* [48], *Tox* [49], and *C1qtnf6* a soluble inhibitor of the alternative complement activation pathway, for which further work is needed to define their functional role.

Transcriptomic analysis of CD8$^+$EGFP$^+$ Treg is to the best of our knowledge the first one to be described. CD8$^+$EGFP$^+$ Treg shared some genes previously described in CD4$^+$EGFP$^+$ Treg, such as *Lrrc32*, *Il2ra*, *Tnfrsf1b*, *Ctla4*, and *Tnfrsf9*, but not other such as *Gata3* [30–35, 45–47]. CD8$^+$EGFP$^+$ Treg expressed immune genes that need to be analyzed for their functional role in Treg. This is the case of complement genes (*C1qc*, *C1qa*, *C1qb*, *Cfd*) and *Fcna* (a secreted molecule with elastin-binding activity), *Hmox1* (enzyme that degrades heme), *Spic* (an enhancer of transcription in lymphoid cells), and *Vipr2* (one of the receptors for vaso-intestinal peptide).

Since there is need to identify cell membrane markers that could allow to purify CD45RC$^{low/-}$CD8$^+$FOXP3$^+$ Treg, several genes that code for membrane markers that were upregulated in CD45RC$^{low/-}$CD8$^+$EGFP$^+$ Treg or in CD45RC$^{low/-}$CD8$^+$EGFP$^-$ Treg were identified that could be used to identify and isolate CD8$^+$EGFP$^+$ Treg by positive or negative selection, respectively. Genes upregulated for cell membrane molecules in CD8$^+$EGFP$^+$ Treg included *Vcam1 (CD106)*, *Cdh1 (CD324)*, *CD163*, *Mrc1 (CD206)*, *Trpm2*, *Kdr (CD309)*, *FcmR*, *Itgb5*, *Il9r (CD129)*, *Il2ra (CD25)*, *Cd79b*, *Ly49s7*, *Jag1 (CD339)*, *Il6st (CD130)*, *IL4r (CD124)*, *Vipr2*, *Tfrc (CD71)*, *Il6r (CD126)* and *Tnfrsf1b (TNFR2)*, *CD44*, and *Icos (CD278)*. In CD8$^+$EGFP$^-$ Treg genes encoding for cell membrane molecules that were upregulated included *Ly49s3*, *Nkg7*, *Ly49s3*, *Fcnb*, *several RT1 (MHC-II) molecules*, *Nrc1 (CD335)*, *Klrk1 (CD314)*, *CD38*, *CD59*, and *CD174*. For this, the RNAseq data need to be confirmed by protein cytometry analyses, as done for CD25, CD44, and ICOS, since not only mRNA levels may not translate into higher protein levels but also because the RNAseq analysis on whole cell populations do not allow to conclude whether it is a large or a small fraction of the cells that upregulate a given gene. Thus, these cell membrane markers could potentially be used to identify and purify CD8$^+$ nTreg in wild-type rats and even in other species. On this regard, human CD8$^+$CD45RC$^{low/-}$ cells contain the CD8$^+$ Treg suppressive activity but further enrichment of cells positives for CD25 or negatives for CD127 did not increase the suppressive activity compared to the total CD8$^+$CD45RC$^{low/-}$ population [7]. This suggest a difference between human and rat nCD8$^+$ Treg for these markers but human CD8$^+$CD45RC$^{low/-}$FOXP3$^+$ cells did express higher levels of GITR than CD8$^+$CD45RC$^{low/-}$FOXP3$^-$ cells and were more suppressive than the GITR$^-$ fraction of CD8$^+$CD45RC$^{low/-}$ cells [7] showing a concordance with the transcriptomic data presented in this manuscript.

In the intestinal epithelium of mice, a small proportion of CD4$^+$ Treg loose expression of *Foxp3* and express CD8alpha [50]. Future experiments in the gut and other organs and tissues will define whether EGFP$^+$ cells co-express CD8 and CD4 markers.

CD4$^+$ and CD8$^+$ iTreg have been described in in vitro and in vivo condititons [1, 3, 4, 6, 7]. In vitro culture Tconv CD4$^+$CD25$^-$ EGFP$^-$ or CD8$^+$CD45RC$^{low/-}$GFP$^-$ cells in the presence of TGFbeta and IL-2 but not of IL-2 alone resulted in the induction of EGFP in a fraction of cells. The suppressive activity of the cultured cells was restricted to the EGFP$^+$ fraction of cells in both CD4$^+$ and CD8$^+$ T cell compartments and these are thus truly iTreg. This suggests that *Foxp3-EGFP* rats could be used to analyze iTreg in different situations in vitro and in vivo. Generation of FOXP3$^+$ cells from CD4$^+$FOXP3$^-$ in humans can be obtained with IL-2 in the absence of TGFbeta but these cells may not be truly Treg since expression of FOXP3 by human cells can be a marker of activation [37]. On the contrary, IL-2 alone in mice does not induce FOXP3$^+$ cells [36]. In both species, mice and human, TGFbeta induces the expression of FOXP3 [36]. Thus, induction of expression of FOXP3 in rat Teg cells could be similar to the one observed in mice and different from the one in human Treg but this needs further experiments with additional stimuli.

Low-dose IL-2 treatment was shown to preferentially expand both CD4+ and CD8+ FOXP3+ Treg in mice [51, 52], non-human primates [38], and humans [39]. In mice, the doses used ranged between 5×10^3 and

5×10^4 IU/g of body weight [51, 53]. The dose of IL-2 used in this study also (10^4 IU/g of body weight) was the same used in a previous study in rats that showed increase in CD4+ Treg but in which CD8+ Treg were not described [40]. Although with this dose of IL-2 we observed a preferential expansion and activation of both $CD4^+$ and $CD8^+$ $EGFP^+$ Treg, we also observed increased $CD4^+$ and $CD8^+$ Tconv and NK cells and thus future experiments could analyze lower doses to define a more restricted effect on Treg. It should be noted that doses of 2×10^3 IU/rat in HLA-B27 with spondyloarthropathy had a weak effect on CD4+ Treg induction [53].

Similar percentages of $CD4^+FOXP3^+$ Treg have been described in different rat strains and $CD4^+$ and $CD8^+$ Treg in rats have been studied in a variety of pathophysiological situations [5, 6]. Although the role of $CD8^+$ Treg is less studied than for $CD4^+$ Treg, there is solid evidence that this subset of Treg plays an important role in immune responses not only in rats but also in all other species analyzed [4, 7, 13, 14, 54].

Conclusions

Foxp3-EGFP rats are a useful model to identify $CD4^+$ and $CD8^+$ Treg and to define new molecules expressed in by $CD4^+$ but particularly $CD8^+$ Treg that will allow to better define their phenotype and function.

The immune system of rats have several characteristics that make them more similar to humans than mice [25] and the recent generation of many gene edited rats [26] will allow to cross *Foxp3-EGFP* rats with other mutated strains to analyze the role of Treg in these models.

Methods

Animals

Wild type Sprague-Dawley (SD/Crl) rats were from Charles River (L'Arbresle, France). *Foxp3-GFP* founder reporter mice were kindly provided by Bernard Malissen [18]. All the animal care and procedures performed in this study were approved by the Animal Experimentation Ethics Committee of the Pays de la Loire region, France, in accordance with the guidelines from the French National Research Council for the Care and Use of Laboratory Animals (Permit Number : Apafis 692). All efforts were made to minimize suffering. The rats were housed in a controlled environment (temperature 21 ± 1 °C, 12-h light/dark cycle).

Generation and genotyping of *Foxp3-EGFP* animals

Several CRISPR sgRNA sequences cleaving immediately 3′ of the stop codon of *Foxp3* were designed using the CRISPOR software. The in vitro transcribed sgRNA were purified and one selected for highest cleavage in the rat C6 cell line, as previously described in detail [55, 56].

Fertilized one-cell stage embryos were collected for subsequent microinjection using a previously published procedure [57]. Briefly, a mixture of Cas9 protein (50 ng/µl), sgRNA (GCAGGGGTTGGAGCACTTGC) (10 ng/µl), and donor DNA (2 ng/µl) encoding the 2A self-cleaving peptide and EGFP sequences flanked by homology arms (1 kb each) 5′ and 3′ from the DNA cleavage point (Fig. 1A) was microinjected both into the male pronucleus and into the cytoplasm of fertilized one-cell stage embryos. Microinjected zygotes were maintained under 5% CO_2 at 37 °C for 2h. Surviving embryos were implanted on the same day in the oviduct of pseudo-pregnant females (0.5 dpc) and allowed to develop to full term.

For genotyping rats, DNA from tail biopsy from 8- to 10-day-old rats were digested in 500 µL of tissue digestion buffer (Tris–HCl 0.1 mol/L pH 8.3, EDTA 5 mmol/L, SDS 0.2%, NaCl 0.2 mol/L, PK 100 µg/mL) in a 1.5 mL tube at 56 °C overnight and genotyped by PCR using the following primers: *Foxp3*-up; 5′-AAC CTG GGG CTA AAT GTG TG-3′; *Foxp3*-low; 5′-TAG GGT TTG GGT TGA GTC CA-3′; *EGFP*-up; 5′-CCT CGT GAC CAC CCT GAC CT-3′; *EGFP*-low; 5′-TCC ATG CCG AGA GTG ATC CC-3′. PCR amplicons were analyzed by capillary electrophoresis as described [58], followed by Sanger sequencing in *Foxp3*-mutated founders.

Cytofluorimetry and antibodies

Single-cell suspensions from the spleen, thymus, bone marrow, and lymph nodes were prepared as described previously [59]. Cell suspensions were analyzed using antibodies (antibodies used are listed in supplementary Table 8). The incubation period was 30 min at 4 °C, and the analysis was performed with a FACSVerse system (BD Biosciences, Franklin Lakes, NJ) and FlowJo software (Tree Star, Ashland, OR).

In vitro suppressive assays

Suppressive assays were performed as previously described in detail [56, 60]. Briefly, $CD4^+CD25^-$ naive T cells, $CD4^+CD25^+CD127^{low}$ and $CD8^+CD45RC^{low/-}$ Treg expressing or not FOXP3 were FACS-sorted from *Foxp3-EGFP* or WT rats (haplotype RT-1u). $CD4^+CD25^-$ responder naive T cells were CPD-670-labeled. $CD4^+CD25^+CD127^{low}$ (labeled with CPD-450 to differentiate them from the responder $CD4^+$ naïve cells) and $CD8^+CD45RC^{low/-}$ T cells were co-cultured at different ratios with $CD4^+CD25^-$ responder naive T cells and spleen DCs from Lew.1A rats (haplotype RT-1a, to

stimulate in a mixed lymphocyte reaction the responder naïve $CD4^+$ T cells from animals with haplotype RT-1u) for 6 days at 37C ° in 5% CO_2. Proliferation of CPD 670-labeled $CD4^+CD25^-$ naive T cells was analyzed by gating $TCR^+CD4^+CPD450^-$ cells (R7/3-APC, OX35-PECY7) among living cells and analyzing CPD-670 signal dilution.

Transcriptomic analysis of $CD8^+$ and $CD4^+$ $EGFP^+$ cells

We isolated $TCR^+CD25^{high}CD127^{low}CD4^+EGFP^+$, $TCR^+CD25^{high}CD127^{low}CD4^+EGFP^-$, $TCR^+CD45RC^{low/-}CD8^+EGFP^+$, and $TCR^+CD45RC^{low/-}CD8^+EGFP^-$ cells and performed total RNAseq by performing 3′Digital Gene Expression (3′DGE) RNA-sequencing. A RNeasy-Mini Kit (Qiagen) were used to isolate total RNA that was then processed for RNA sequencing. Protocol of 3′digital gene expression (3′DGE) RNA-sequencing was performed as previously described [7]. Briefly, the libraries were prepared from 10 ng of total RNA. The mRNA poly(A) tail is tagged with well specific barcodes and unique molecular identifier (UMI) and flanked by universal sequencing adapters during the template-switching reverse transcriptions.

Barcoded cDNAs from multiple samples are then pooled, amplified, and tagmented using a transposon-fragmentation approach which enriches for 3′ ends of cDNA. A library of 350–800 bp is sequenced on a S1 flowcell on a NovaSeq 6000 (Illumina). Digital gene expression (DGE) profiles are generated by counting for each sample the number of unique UMIs associated with each RefSeq genes. Counts matrix was normalized by a linear model with the R package DESeq2 [61]. Differential gene expression was determined Wald test and corrected with the false discovery rate (FDR) multiple testing method. Genes were considered differentially expressed if the FDR <= 0.05 and the absolute value of $\log_2$(Fold Change) greater than 0.5. Heatmaps were generated with the R package gplots (https://cran.r-project.org/web/packages/gplots/index.html); Volcano plots were drawn by plotting -log10 (FDR) in function of log2(Fold-Change).

Genes were highlighted when absolute value of log2(Fold-Change) was superior to 1 and FDR <= to 0.05. Principal component analyses (PCA) and confident ellipses were generated with the function coord.ellipse from the R package FactoMineR [62] with default parameters. Both pathways from the Kyoto Encyclopedia of genes and genomes (KEGG) [63] as well as gene ontologies (GO) [64] were tested for enrichment among differentially expressed genes with the R package clusterProfiler [65]. The significant GO terms and their enrichment scores were filtered with a corrected *P*-value <= 0.05 (Benjamini-Hochberg method).

In vitro generated $EGFP^+$ induced Tregs

$EGFP^-CD4^+CD25^-$ and $EGFP^-CD8^+CD45RC^{low/-}$ T cells were FACS-sorted from *Foxp3-EGFP* rats, labeled with CPD 670 and cultured for 3 days in the presence of anti-CD3 and anti-CD28 MAbs with different doses of hTGFbeta (0, 5, 20 µg/ml) and with or without 100 IU of hIL-2 at 37 °C in 5% CO_2. Proliferation of CPD-labeled T cells measured by dilution of the CPD signal and EGFP expression were analyzed using a FACSVerse system (BD Biosciences, Franklin Lakes, NJ) and FlowJo software (Tree Star, Ashland, OR). $EGFP^+$ $CD4^+$ and $CD8^+$ cells as well as $EGFP^-$ $CD4^+$ and $CD8^+$ cells were sorted at the end of the culture period and used in suppressive assays as described in a section above. Sorted $EGFP^+$ cells were also permeabilized, fixed, and analyzed for expression of FOXP3 using anti-FOXP3 antibodies.

IL-2 expansion of $EGFP^+$ Tregs in vivo

Human IL-2 (Proleukin) was diluted with NaCl for iv injection; a new dilution was used for each day of treatment, at a dose (10^4 IU/0.62 µg/g of body weight for 4 consecutive days) previously described to expand Treg in rats [37], and analyzed at day 5; the proportion and absolute numbers of NK, $CD4^+EGFP^-$ Tconv, $CD4^+EGFP^+$ Treg, $CD8^+$EGFP- Tconv, and $CD8^+EGFP^+$ Treg cells in blood and spleen as well as the expression levels of Stat-5 phosphorylation (clone pY694, BD Biosciences) and CD25 (clone OX39) were compared to those of these cell populations from untreated *Foxp3-EGFP* rats.

Statistical analysis

Results are presented as means ± SEM. Statistical analysis between samples was performed by a Mann-Whitney test using GraphPad Prism 4 software (GraphPad Software, San Diego, CA, USA). Differences associated with probability values of $^aP < 0.05$, $^bP < 0.005$, $^cP < 0.0002$, and $^dP < 0.0001$ were considered statistically significant.

Supplementary Information

The online version contains supplementary material available at https://doi.org/10.1186/s12915-022-01502-0.

Additional file 1: Supplementary figure 1. Flow cytometry analyses of spleen and thymus cells from *Foxp3-EGFP* rats. A) Spleen, thymus and bone marrow were harvested from 12 weeks-old *Foxp3-EGFP* or wild-type (WT) rats and single cell suspensions were gated by SSC and FSC on lymphocytes followed by the identification with mAbs of major cell populations such as TCR^+ cells (TCR^+CD4^+, TCR^+CD8^+), TCR^- cells (TCR-CD4+ and TCR-CD8+) and $CD161^+$ for NK cells. These populations were then analyzed for FOXP3 expression by EGFP expression and by using an anti-FOXP3 mAb. Contour plots from one animal representative of 6 analyzed in the same conditions. Right hand graphs are the mean and SEM of all animals analyzed. Student's t test $^*P < 0.05$, $^{**}P < 0.01$, $^{***}P < 0.001$, and $^{****}P < 0.0001$. B) PBMCs from WT and *Foxp3*$^{-}$*EGFP*$^{+}$ rats were analyzed using untreated (left panels) or permeabilized and fixed (2 middle panels) cells with the conditions used for the analysis using

anti-FOXP3 antibodies. Compared to untreated cells, EGFP signals were reduced in permeabilized cells, as previously described [59]. Co-labeling using anti-FOXP3 antibodies and EGFP in permeabilized cells (2 right panels) showed co-staining in $CD4^+$ and $CD8^+$ T cells from *Foxp3-EGFP* animals. C. $EGFP^+$ cells were sorted from spleen, permeabilized and fixed followed by analysis using anti-FOXP3 antibodies. All sorted $EGFP^+$ cells expressed FOXP3. **Supplementary figure 2.** Suppression assay using T $CD4^+EGFP^+$ and $CD8^+EGFP^+$ cells. Representative histograms of a suppressive assay using spleen cells from 12 weeks-old *Foxp3-EGFP* rats. TCR $^+CD4^+CD25^+CD127^{low}EGFP^+$ (labeled with CPD-450) responder cells and $TCR^+CD8^+CD45RC^{low/-}EGFP^+$ cells were sorted and added to an MLR in a 1:1 or 1:0.5 Tresponder to Tregs cells. The MLR was performed by co-culturing in a 1:1 ratio spleen $CD4^+CD25^-$ Tconv cells from SPD rats (MHC haplotype u) labeled with CPD-670 along with enriched spleen APCs from Lewis 1A (MHC haplotype a) rats. Decrease in the percentage of CPD-670 bright cells and increase in the percentages of CPD-670 low cells denote dilution of CPD-670 with cell proliferation. The right histogram shows the CPD-670 dilution of proliferating T cells in the absence of Treg and the others show less proliferation in the presence of the $EGFP^+$ Treg. Representative experiment out of 4 performed. **Supplementary figure 3.** RNAseq analyses of $EGFP^+$ and $EGFP^-$ within $CD4^+$ and $CD8^+$ T cells. TCR $^+CD25^{high}CD127^{low}CD4^+$ and $TCR^+CD45RC^{low/-}$ $CD8^+$ $EGFP^+$ and $EGFP^-$ T cells were cell sorted and RNAseq analyses were performed comparing $CD4^+EGFP^+$ vs. $CD4^+EGFP^-$ cells, and $CD8^+EGFP^+$ vs. $CD8^+EGFP^-$ cells and $CD8^+EGFP^+$ vs. $CD4^+EGFP^+$ cells. A. R-Shiny representations of RNAseq levels for individual samples of the indicated genes with immune functions expressed in units per million reads. B. GO analyses of analysis of functional pathways, Cell component analysis showed that the proteins encoded by comparison of $TCR^+CD25^{high}CD127^{low}CD4^+EGFP^+$ vs. TCR $^+CD25^{high}CD127^{low}CD4^+EGFP^-$, $TCR^+CD45RC^{low/-}CD8^+EGFP^+$ vs. TCR $^+CD45RC^{low/-}CD8^+EGFP^-$ and $TCR^+CD25^{high}CD127^{low}CD4^+EGFP^+$ vs. TCR $^+CD45RC^{low/-}CD8^+EGFP^+$ cells. (a) Comparison of 5 principal pathways in immune cell activation (b) Comparison of 3 principal pathway in immune cell proliferation. (c) Comparison of 4 principal pathway in immune cell adhesion. (d) Comparison of 11 pathways in miscellaneous process. C. Venn diagrams showing the overlap in genes that were significantly (adjusted *P* value, 0.05 and absolute log2 fold-change of genes differentially upregulated (left) or down regulated (right). D. Heatmap analysis of DEG grouped together for all $CD4^+EGFP^+$ vs. $CD4^+EGFP^-$ cells, $CD8^+EGFP^+$ vs. $CD8^+EGFP^-$ cells, as well as $CD4^+EGFP^+$ cells vs. $CD8^+EGFP^+$ cells. **Supplementary figure 4.** Confirmation of RNAseq results on CD4+EGFP+ and CD8+EGFP+ cells by FACS. A. Histograms of TCR+CD4+EGFP+, TCR+CD4+EGFP-, TCR+CD8+EGFP+and TCR+CD8+EGFP- cells analyzed with the indicate mAbs. Percentages above the traits correspond to the number of positive cells above staining with isotype control mAbs. One experiment representative of 4 performed in the same conditions. Lower graphs are the mean and SEM f all animals analyzed. Student's t test $*P < 0.05$, $**P < 0.01$, $***P < 0.001$, and $****P < 0.0001$. B. R-Shiny representation of RNAseq expression levels expressed in individual sample in units per million reads for *Il2ra (Cd25)*, *Cd44* and *Icos*. **Supplementary figure 5.** Analysis using anti-FOXP3 antibodies of $EGFP^+$ cells induced in vitro. Spleen cells from *Foxp3*-EGFP animals were used to sort Tconv CD4+CD25-$EGFP^-$ Treg and T CD8+CD45RClow/-EGFP- cells and cultured for 3 days in the presence of anti-CD3/CD28 mAbs, IL-2 and in the absence or presence of hTGFbeta. $CD4^+$ or $CD8^+$ $EGFP^+$ cells were cell sorted, permeabilized, fixed and analyzed using anti-FOXP3 antibodies. Results show that all EGFP+ cells were also anti-FOXP3+ cells ($n = 3$). graphs are the mean and SEM of all animals analyzed. Student's t test $*P < 0.05$, $**P < 0.01$, $***P < 0.001$, and $****P < 0.0001$. **Supplementary figure 6.** IL-2 induce expansion of $EGFP^+$ Tregs in spleen. *Foxp3-EGFP* rats received or not hIL-2 at low doses and the percent of the indicated cell populations was analyzed in spleen. Percentages of cells in the indicated cell populations of IL-2-treated and untreated rats. Left graph shows mean ± SEM, $n = 3$, and right contour plots show a representative animal. **Supplementary figure 7.** $CD4^+$ and $CD8^+$ $FOXP3^+$ Treg in *Foxp3-EGFP* mice. Lymphocytes (PBL) and spleen cells from *Foxp3-EGFP* mice were analyzed for the expression of EGFP+ cells as well as for FOXP3+ cells using antibodies among CD4+ and CD8+ T cells. Graphs show mean ± SEM and each point represents an individual animal. **Table S1.** Frequency of $CD4^+EGFP^+$ and $CD8^+EGFP^+$ in *Foxp3-EGFP* rats and *Foxp3-EGFP* mice. **Table S2.** Immune genes upregulated in TCD4+EGFP+ vs. TCD4+EGFP- cells. **Table S3.** Immune genes upregulated in TCD8+EGFP+ vs. TCD8+EGFP- cells. **Table S4.** Immune genes upregulated in CD4+EGFP+ vs. CD8+EGFP+ cells. **Table S5.** Genes that are upregulated in Venn diagrams. **Table S6.** Genes that are downregulated in Venn diagrams. **Table S6.** Unique genes (333) in CD8+EGFP+ vs. CD8+EGFP- Treg. **Table S6.** Common genes (24) between CD4+EGFP+ vs. CD4+EGFP- cells and CD8+EGFP+ vs. CD8+EGFP- cells. **Table S6.** Unique genes (212) between CD4+EGFP+ vs. CD8+EGFP+ Treg. **Table S6.** Common genes (24) between CD4+EGFP+ vs. CD8+EGFP+ cells. **Table S6.** Common genes (3) between CD4+EGFP+ vs. CD8+EGFP+ and CD8+EGFP+ vs. CD8+EGFP- cells and CD4+EGFP+ vs. CD4+EGFP- cells. **Table S6.** Common genes (3) between CD4+EGFP+ vs. CD8+EGFP+ and CD8+EGFP+ vs. CD8+EGFP- and CD4+EGFP+ vs. CD4+EGFP- cells. **Table S7.** Increase in different EGFP+ and EGFP- cell subsets in blood following IL-2 treatment. **Table S8.** Antibodies used in the study.

Acknowledgements
This work was realized in the context of different programs: Biogenouest by Région Pays de la Loire, IBiSA program, TEFOR (Investissements d'Avenir French Government program, ANRII-INSB-0014), LabCom SOURIRAT project (ANR-14-LAB5-0008), Labex IGO project (Investissements d'Avenir French Government program, ANR-11-LABX-0016-01), IHU-Cesti project (Investissements d'Avenir French Government program, ANR-10-IBHU-005, Nantes Métropole and Région Pays de la Loire), and Fondation Progreffe. We acknowledge Bernard Malissen and Cédric Louvet for providing the *Foxp3-GFP* mice.

Authors' contributions
All authors read and approved the final manuscript. SM designed and performed the research, analyzed the data, and edited the manuscript. LT performed the research, analyzed the data, and edited the manuscript. SR, VG, CS, CU, AG, VC, L-HO, MG, J-MH, and CF performed the research and analyzed the data. CG and JP analyzed the data and edited the manuscript. IA designed the research, provided the funding, analyzed the data, and wrote the manuscript.

Funding
This work was supported by different programs: Biogenouest by Région Pays de la Loire, IBiSA program, TEFOR (Investissements d'Avenir French Government program, ANRII-INSB-0014), LabCom SOURIRAT project (ANR-14-LAB5-0008), Labex IGO project (Investissements d'Avenir French Government program, ANR-11-LABX-0016-01), IHU-Cesti project (Investissements d'Avenir French Government program, ANR-10-IBHU-005, Nantes Métropole and Région Pays de la Loire), and Fondation Progreffe.

Availability of data and materials
The sequencing data have been available from the NCBI GEO database, under accession GSE189797 [66]. Graphical representations were created with R packages [65].

Declarations

Ethics approval and consent to participate
All experiments were procedures were approved by the Animal Experimentation Ethics Committee of the Pays de la Loire region, France, in accordance with the guidelines from the French National Research Council for the Care and Use of Laboratory Animals.

Consent for publication
Not applicable.

Competing interests
The authors declare that they have no competing interests.

Received: 9 September 2022 Accepted: 16 December 2022
Published online: 12 January 2023

References

1. Sakaguchi S, Yamaguchi T, Nomura T, et al. Regulatory T cells and immune tolerance. Cell. 2008;133(5):775–87. https://doi.org/10.1016/j.cell.2008.05.009.
2. Sakaguchi S, Sakaguchi N, Asano M, et al. Immunologic self-tolerance maintained by activated T cells expressing IL-2 receptor alpha-chains (CD25). Breakdown of a single mechanism of self-tolerance causes various autoimmune diseases. J Immunol. 1995;155(3):1151–64.
3. Attias M, Al-Aubodah T, Piccirillo CA. Mechanisms of human FoxP3(+) Treg cell development and function in health and disease. Clin Exp Immunol. 2019;197(1):36–51. https://doi.org/10.1111/cei.13290.
4. Flippe L, Bezie S, Anegon I, et al. Future prospects for CD8(+) regulatory T cells in immune tolerance. Immunol Rev. 2019;292(1):209–24. https://doi.org/10.1111/imr.12812.
5. Rodriguez-Perea AL, Arcia ED, Rueda CM, et al. Phenotypical characterization of regulatory T cells in humans and rodents. Clin Exp Immunol. 2016;185(3):281–91. https://doi.org/10.1111/cei.12804.
6. Bezie S, Anegon I, Guillonneau C. Advances on CD8+ Treg cells and their potential in transplantation. Transplantation. 2018;102(9):1467–78. https://doi.org/10.1097/TP.0000000000002258.
7. Bezie S, Meistermann D, Boucault L, et al. Ex vivo expanded human non-cytotoxic CD8(+)CD45RC(low/-) Tregs efficiently delay skin graft rejection and GVHD in humanized mice. Front Immunol. 2017;8:2014. https://doi.org/10.3389/fimmu.2017.02014.
8. Roncarolo MG, Gregori S, Bacchetta R, et al. The biology of T regulatory type 1 cells and their therapeutic application in immune-mediated diseases. Immunity. 2018;49(6):1004–19. https://doi.org/10.1016/j.immuni.2018.12.001.
9. Singh RP, Hahn BH, Bischoff DS. Cellular and molecular phenotypes of pConsensus peptide (pCons) induced CD8+ and CD4+ regulatory T cells in lupus. Front Immunol. 2021;12:718359. https://doi.org/10.3389/fimmu.2021.718359.
10. Singh RP, Bischoff DS, Hahn BH. CD8+ T regulatory cells in lupus. Rheumatol Immunol Res. 2021;2(3):147–56. https://doi.org/10.2478/rir-2021-0021.
11. Siegmund K, Rückert B, Ouaked N, et al. Unique phenotype of human tonsillar and in vitro-induced FOXP3+CD8+ T cells. J Immunol. 2009;182(4):2124–30. https://doi.org/10.4049/jimmunol.0802271.
12. Lim A, French MA, Price P. CD4+ and CD8+ T cells expressing FoxP3 in HIV-infected patients are phenotypically distinct and influenced by disease severity and antiretroviral therapy. J Acquir Immune Defic Syndr. 2009;51(3):248–57. https://doi.org/10.1097/QAI.0b013e3181a74fad.
13. Guillonneau C, Hill M, Hubert FX, et al. CD40lg treatment results in allograft acceptance mediated by CD8CD45RC T cells, IFN-gamma, and indoleamine 2,3-dioxygenase. J Clin Invest. 2007;117(4):1096–106. https://doi.org/10.1172/JCI28801.
14. Bezie S, Charreau B, Vimond N, et al. Human CD8+ Tregs expressing a MHC-specific CAR display enhanced suppression of human skin rejection and GVHD in NSG mice. Blood Adv. 2019;3(22):3522–38. https://doi.org/10.1182/bloodadvances.2019000411.
15. Xystrakis E, Bernard I, Dejean AS, et al. Alloreactive CD4 T lymphocytes responsible for acute and chronic graft-versus-host disease are contained within the CD45RChigh but not the CD45RClow subset. Eur J Immunol. 2004;34(2):408–17. https://doi.org/10.1002/eji.200324528.
16. Xystrakis E, Dejean AS, Bernard I, et al. Identification of a novel natural regulatory CD8 T-cell subset and analysis of its mechanism of regulation. Blood. 2004;104(10):3294–301. https://doi.org/10.1182/blood-2004-03-1214.
17. Vimond N, Lasselin J, Anegon I, et al. Genetic engineering of human and mouse CD4(+) and CD8(+) Tregs using lentiviral vectors encoding chimeric antigen receptors. Mol Ther Methods Clin Dev. 2021;20:69–85. https://doi.org/10.1016/j.omtm.2020.11.008.
18. Wang Y, Kissenpfennig A, Mingueneau M, et al. Th2 lymphoproliferative disorder of LatY136F mutant mice unfolds independently of TCR-MHC engagement and is insensitive to the action of Foxp3+ regulatory T cells. J Immunol. 2008;180(3):1565–75. https://doi.org/10.4049/jimmunol.180.3.1565.
19. Fontenot JD, Rasmussen JP, Gavin MA, et al. A function for interleukin 2 in Foxp3-expressing regulatory T cells. Nat Immunol. 2005;6(11):1142–51. https://doi.org/10.1038/ni1263.
20. Haribhai D, Lin W, Relland LM, et al. Regulatory T cells dynamically control the primary immune response to foreign antigen. J Immunol. 2007;178(5):2961–72. https://doi.org/10.4049/jimmunol.178.5.2961.
21. Lin W, Haribhai D, Relland LM, et al. Regulatory T cell development in the absence of functional Foxp3. Nat Immunol. 2007;8(4):359–68. https://doi.org/10.1038/ni1445.
22. Rubtsov YP, Rasmussen JP, Chi EY, et al. Regulatory T cell-derived interleukin-10 limits inflammation at environmental interfaces. Immunity. 2008;28(4):546–58. https://doi.org/10.1016/j.immuni.2008.02.017.
23. Wan YY, Flavell RA. Identifying Foxp3-expressing suppressor T cells with a bicistronic reporter. Proc Natl Acad Sci U S A. 2005;102(14):5126–31. https://doi.org/10.1073/pnas.0501701102.
24. Bettelli E, Carrier Y, Gao W, et al. Reciprocal developmental pathways for the generation of pathogenic effector TH17 and regulatory T cells. Nature. 2006;441(7090):235–8. https://doi.org/10.1038/nature04753.
25. Wildner G. Are rats more human than mice? Immunobiology. 2019;224(1):172–6. https://doi.org/10.1016/j.imbio.2018.09.002.
26. Chenouard V, Remy S, Tesson L, et al. Advances in genome editing and application to the generation of genetically modified rat models. Front Genet. 2021;12:615491. https://doi.org/10.3389/fgene.2021.615491.
27. Breban M, Araujo LM, Chiocchia G. Animal models of spondyloarthritis: do they faithfully mirror human disease? Arthritis Rheum. 2014;66(7):1689–92. https://doi.org/10.1002/art.38636.
28. Ossart J, Moreau A, Autrusseau E, et al. Breakdown of immune tolerance in AIRE-deficient rats induces a severe autoimmune polyendocrinopathy-candidiasis-ectodermal dystrophy-like autoimmune disease. J Immunol. 2018;201(3):874–87. https://doi.org/10.4049/jimmunol.1701318.
29. Kalejta RF, Shenk T, Beavis AJ. Use of a membrane-localized green fluorescent protein allows simultaneous identification of transfected cells and cell cycle analysis by flow cytometry. Cytometry. 1997;29(4):286–91. https://doi.org/10.1002/(sici)1097-0320(19971201)29:4<286::aid-cyto4>3.0.co;2-8
30. Bhairavabhotla R, Kim YC, Glass DD, et al. Transcriptome profiling of human FoxP3+ regulatory T cells. Hum Immunol. 2016;77(2):201–13. https://doi.org/10.1016/j.humimm.2015.12.004.
31. van der Veeken J, Arvey A, Rudensky A. Transcriptional control of regulatory T-cell differentiation. Cold Spring Harb Symp Quant Biol. 2013;78:215–22. https://doi.org/10.1101/sqb.2013.78.020289.
32. Pfoertner S, Jeron A, Probst-Kepper M, et al. Signatures of human regulatory T cells: an encounter with old friends and new players. Genome Biol. 2006;7(7):R54. https://doi.org/10.1186/gb-2006-7-7-r54.
33. Hollbacher B, Duhen T, Motley S, et al. Transcriptomic profiling of human effector and regulatory T cell subsets identifies predictive population signatures. Immunohorizons. 2020;4(10):585–96. https://doi.org/10.4049/immunohorizons.2000037.
34. Worthington JJ, Kelly A, Smedley C, et al. Integrin alphavbeta8-mediated TGF-beta activation by effector regulatory T cells is essential for suppression of T-cell-mediated inflammation. Immunity. 2015;42(5):903–15. https://doi.org/10.1016/j.immuni.2015.04.012.
35. Probst-Kepper M, Geffers R, Kroger A, et al. GARP: a key receptor controlling FOXP3 in human regulatory T cells. J Cell Mol Med. 2009;13(9B):3343–57. https://doi.org/10.1111/j.1582-4934.2009.00782.x.
36. Fantini MC, Becker C, Monteleone G, et al. Cutting edge: TGF-beta induces a regulatory phenotype in CD4+CD25- T cells through Foxp3 induction and down-regulation of Smad7. J Immunol. 2004;172(9):5149–53. https://doi.org/10.4049/jimmunol.172.9.5149.
37. Walker MR, Kasprowicz DJ, Gersuk VH, et al. Induction of FoxP3 and acquisition of T regulatory activity by stimulated human CD4+CD25- T cells. J Clin Invest. 2003;112(9):1437–43. https://doi.org/10.1172/JCI19441.
38. Aoyama A, Klarin D, Yamada Y, et al. Low-dose IL-2 for in vivo expansion of CD4+ and CD8+ regulatory T cells in nonhuman primates. Am J Transplant. 2012;12(9):2532–7. https://doi.org/10.1111/j.1600-6143.2012.04133.x.
39. Rosenzwajg M, Churlaud G, Mallone R, et al. Low-dose interleukin-2 fosters a dose-dependent regulatory T cell tuned milieu in T1D patients. J Autoimmun. 2015;58:48–58. https://doi.org/10.1016/j.jaut.2015.01.001.
40. Weishaupt A, Paulsen D, Werner S, et al. The T cell-selective IL-2 mutant AIC284 mediates protection in a rat model of multiple sclerosis. J Neuroimmunol. 2015;282:63–72. https://doi.org/10.1016/j.jneuroim.2015.03.020.

41. Goldstein JD, Balderas RS, Marodon G. Continuous activation of the CD122/STAT-5 signaling pathway during selection of antigen-specific regulatory T cells in the murine thymus. PLoS One. 2011;6(4):e19038. https://doi.org/10.1371/journal.pone.0019038.
42. Ward NC, Yu A, Moro A, et al. IL-2/CD25: a long-acting fusion protein that promotes immune tolerance by selectively targeting the IL-2 receptor on regulatory T cells. J Immunol. 2018;201(9):2579–92. https://doi.org/10.4049/jimmunol.1800907.
43. Li Z, Lin F, Zhuo C, et al. PIM1 kinase phosphorylates the human transcription factor FOXP3 at serine 422 to negatively regulate its activity under inflammation. JBC. 2014;289(39):268721–26881. https://doi.org/10.1074/jbc.M114.586651.
44. Lin F, Luo X, Tsun A, et al. Kaempferol enhances the suppressive function of Treg cells by inhibiting FOXP3 phosphorylation. Int Immunopharmacol. 2015;28(2):859–65. https://doi.org/10.1016/j.intimp.2015.03.044.
45. Cuadrado E, van den Biggelaar M, de Kivit S, et al. Proteomic analyses of human regulatory T cells reveal adaptations in signaling pathways that protect cellular identity. Immunity. 2018;48(5):1046–1059 e6. https://doi.org/10.1016/j.immuni.2018.04.008.
46. Dombrowski Y, O'Hagan T, Dittmer M, et al. Regulatory T cells promote myelin regeneration in the central nervous system. Nat Neurosci. 2017;20(5):674–80. https://doi.org/10.1038/nn.4528.
47. Schiering C, Krausgruber T, Chomka A, et al. The alarmin IL-33 promotes regulatory T-cell function in the intestine. Nature. 2014;513(7519):564–8. https://doi.org/10.1038/nature13577.
48. Muraoka D, Seo N, Hayashi T, et al. Signal-transducing adaptor protein-2 promotes generation of functional long-term memory CD8+ T cells by preventing terminal effector differentiation. Oncotarget. 2017;8(19):30766–80. https://doi.org/10.18632/oncotarget.15403.
49. Khan O, Giles JR, McDonald S, et al. TOX transcriptionally and epigenetically programs CD8(+) T cell exhaustion. Nature. 2019;571(7764):211–8. https://doi.org/10.1038/s41586-019-1325-x.
50. Bilate AM, London M, Castro TBR, et al. T cell receptor is required for differentiation, but not maintenance, of intestinal CD4+ intraepithelial lymphocytes. Immunity. 2020;53(5):1001–14. https://doi.org/10.1016/j.immuni.2020.09.003.
51. Abbas AK, Trotta EDRS, Marson A, et al. Revisiting IL-2: biology and therapeutic prospects. Sci Immunol. 2018;3(25):eaat 1482. https://doi.org/10.1126/sciimmunol.aat1482.
52. Churlaud G, Pitoiset F, Jebbawi F, et al. Human and mouse CD8(+) CD25(+)FOXP3(+) regulatory T cells at steady state and during interleukin-2 therapy. Front Immunol. 2015;6:171. https://doi.org/10.3389/fimmu.2015.00171.
53. Araujo LM, Jouhault Q, Fert I, et al. Effects of a low-dose IL-2 treatment in HLA-B27 transgenic rat model of spondyloarthritis. Arthritis Res Ther. 2021;23(1):193. https://doi.org/10.1186/s13075-021-02559-y.
54. Bezie S, Picarda E, Tesson L, et al. Fibrinogen-like protein 2/fibroleukin induces long-term allograft survival in a rat model through regulatory B cells. PLoS One. 2015;10(3):e0119686. https://doi.org/10.1371/journal.pone.0119686.
55. Remy S, Chenouard V, Tesson L, et al. Generation of gene-edited rats by delivery of CRISPR/Cas9 protein and donor DNA into intact zygotes using electroporation. Sci Rep. 2017;7(1):16554. https://doi.org/10.1038/s41598-017-16328-y.
56. Charpentier M, Khedher AHY, Menoret S, et al. CtIP fusion to Cas9 enhances transgene integration by homology-dependent repair. Nat Commun. 2018;9(1):1133. https://doi.org/10.1038/s41467-018-03475-7.
57. Remy S, Tesson L, Menoret S, et al. Efficient gene targeting by homology-directed repair in rat zygotes using TALE nucleases. Genome Res. 2014;24(8):1371–83. https://doi.org/10.1101/gr.171538.113.
58. Chenouard V, Brusselle L, Heslan JM, et al. A rapid and cost-effective method for genotyping genome-edited animals: a heteroduplex mobility assay using microfluidic capillary electrophoresis. J Genet Genomics. 2016;43(5):341–8. https://doi.org/10.1016/j.jgg.2016.04.005.
59. Menoret S, Iscache AL, Tesson L, et al. Characterization of immunoglobulin heavy chain knockout rats. Eur J Immunol. 2010;40(10):2932–41. https://doi.org/10.1002/eji.201040939.
60. Li XL, Menoret S, Bezie S, et al. Mechanism and localization of CD8 regulatory T cells in a heart transplant model of tolerance. J Immunol. 2010;185(2):823–33. https://doi.org/10.4049/jimmunol.1000120.
61. Love MI, Huber W, Anders S. Moderated estimation of fold change and dispersion for RNA-seq data with DESeq2. Genome Biol. 2014;15(12):550. https://doi.org/10.1186/s13059-014-0550-8.
62. version 4.0.3 RCT. A language and environment for statistical computing. R Foundation for Statistical Computing. https://www.R-projectorg. 2020.
63. Kanehisa M, Goto S. KEGG: Kyoto encyclopedia of genes and genomes. Nucleic Acids Res. 2000;28(1):27–30. https://doi.org/10.1093/nar/28.1.27.
64. Ashburner M, Ball CA, Blake JA, et al. Gene ontology: tool for the unification of biology. The Gene Ontology Consortium. Nat Genet. 2000;25(1):25–9. https://doi.org/10.1038/75556.
65. Wu M, Qin X, Ma S. GEInter: an R package for robust gene-environment interaction analysis. Bioinformatics. 2021;37(20):3691–2. https://doi.org/10.1093/bioinformatics/btab318.
66. Anegon I, Ménoret S, Gourain V. RNAseq analysis of CD4+EGFP+ and CD8+EGFP+ regulatory T cells. NCBI GEO accession GSE189797. 2022. https://www.ncbi.nlm.nih.gov/geo/query/acc.cgi?acc=GSE189797.

Publisher's Note